Role of the microcin B17 propeptide in substrate recognition: solution structure and mutational analysis of $McbA_{1-26}$

Ranabir Sinha Roy[1], Soyoun Kim[2], James D Baleja[2] and Christopher T Walsh[1]

Background: The peptide antibiotic microcin B17 (MccB17) contains oxazole and thiazole heterocycles formed by the post-translational modification of four cysteine and four serine residues. An amino-terminal propeptide targets the 69 amino acid precursor of MccB17 (preproMccB17) to the heterocyclization enzyme MccB17 synthetase. The mode of synthetase recognition has been unclear, because there has been limited structural information available on the MccB17 propeptide to date.

Results: The solution structure of the MccB17 propeptide ($McbA_{1-26}$), determined using nuclear magnetic resonance, reveals that $McbA_{1-26}$ is an amphipathic α helix. Mutational analysis of 13 propeptide residues showed that Phe8 and Leu12 are essential residues for MccB17 synthetase recognition. A domain of the propeptide was putatively identified as the region that interacts with the synthetase.

Conclusions: MccB17 synthetase recognizes key hydrophobic residues within a helical propeptide, allowing the selective heterocyclization of downstream cysteine and serine residues in preproMccB17. The determination of the solution structure of the propeptide should facilitate the investigation of other functions of the propeptide, including a potential role in antibiotic secretion.

Addresses: [1]Department of Biological Chemistry and Molecular Pharmacology, Harvard Medical School, Boston, MA 02115, USA. [2]Department of Biochemistry, Tufts University School of Medicine, Boston, MA 02111, USA.

Correspondence: Christopher T Walsh
E-mail: walsh@walsh.med.harvard.edu

Key words: leader, microcin B17, mutagenesis, nuclear magnetic resonance, propeptide

Received: **5 February 1998**
Revisions requested: **27 February 1998**
Revisions received: **13 March 1998**
Accepted: **23 March 1998**

Published: **14 April 1998**

Chemistry & Biology April 1998, 5:217–228
http://biomednet.com/elecref/1074552100500217

Introduction

Microcin B17 (MccB17) belongs to a group of small (<10 kDa) ribosomally encoded antibiotics secreted in the stationary phase by several strains of Enterobacteriaceae [1]. These antibiotics are typically derived from a precursor polypeptide consisting of an amino-terminal leader (propeptide) linked to a carboxy-terminal domain that is often post-translationally modified [2,3]. For MccB17, two Gly–Cys, two Gly–Ser, a Gly–Ser–Cys and a Gly–Cys–Ser sequence in the 69 amino acid precursor polypeptide (preproMccB17) encoded by the *mcbA* structural gene [4] are converted to two thiazoles, two oxazoles, and the bis-heterocyclic 4,2-fused oxazole–thiazoles/thiazole–oxazoles, respectively, by the *mcbBCD* gene products that constitute the microcin B17 synthetase complex (Figure 1) [5–8]. The amino-terminal leader sequence ($McbA_{1-26}$) is subsequently cleaved and the mature 43 amino acid heterocyclic antibiotic comprising residues 27–69 (MccB17) is secreted by an export mechanism using the *mcbEF* gene products [9] that show homology to the ATP-binding cassette (ABC) family of transport proteins [10]. Self-immunity to MccB17 (a putative inhibitor of DNA gyrase) is conferred to the producer strain by *mcbG*, the seventh gene in the MccB17 operon [11,12], by an as yet undetermined mechanism.

Consistent with antibiotic export occurring through a dedicated ABC transport apparatus, the $McbA_{1-26}$ propeptide bears little resemblance to typical signal sequences involved in *sec*-mediated secretion [13]. Instead, the propeptide serves as a prime determinant for the recognition and recruitment of preproMccB17 by MccB17 synthetase [8,14]. In this capacity, the microcin propeptide is similar to the γ-carboxylation site (γ-CRS) propeptides in blood coagulation preproteins [15,16] that recruit vitamin K-dependent γ-glutamyl carboxylase for the post-translational carboxylation of 10–12 downstream glutamic acid residues [17]. Amino-terminal propeptides that are cleaved when peptide antibiotics are secreted are also found in bacteriocins secreted by gram positive bacteria, such as the lantibiotics nisin, subtilin and salivaricin A [2,18]. Although the precise functions of these bacteriocin propeptides are unclear, the propeptides might be involved in the post-translational modification, stabilization and signal-sequence independent secretion of the corresponding prepeptides [2].

Although the MccB17 propeptide is known to be essential for substrate recognition by the synthetase, it is also reminiscent of the double-glycine-type leader peptides [19] that direct the secretion of non-lantibiotics, such as colicin V, by ABC transporters. A knowledge of the three-dimensional structure of the MccB17 propeptide would therefore provide an insight into other biological functions that may be served by this type of prosequence. Here, we present the solution structure of the MccB17 propeptide ($McbA_{1-26}$), and structure-based mutational analysis of this

Figure 1

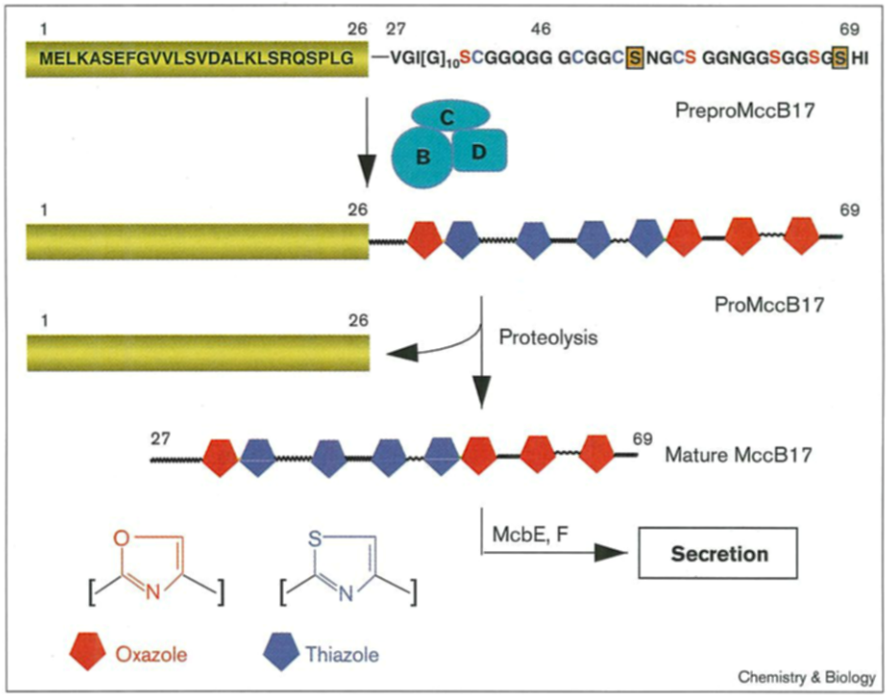

Maturation pathway of microcin B17. The 69 amino acid structural gene product (McbA, preproMccB17) is ribosomally synthesized. An amino-terminal propeptide ($McbA_{1-26}$, yellow) targets preproMccB17 for processing by the heterotrimeric McbB,C,D synthetase complex. Four serine (red) and four cysteine (blue) residues in the downstream sequence ($McbA_{27-69}$) are post-translationally modified to oxazole and thiazole heterocycles respectively (proMccB17). Two serine residues in this domain (orange boxes) remain unprocessed. The propeptide is cleaved by an unknown protease and the mature 43 amino acid polyheterocyclic antibiotic (MccB17) is secreted.

sequence to determine residues essential for recognition by the heterotrimeric McbB,C,D synthetase.

Results

Preliminary structural analysis of the MccB17 propeptide

Primary sequence analysis [20] of preproMccB17 indicated residues 1–20 have a helical conformation. Consistent with this prediction, the circular dichroism (CD) spectrum of a synthetic $McbA_{1-26}$ propeptide (with free amino and carboxyl termini, $McbA_{1-26}$-COOH) at physiological pH showed distinctive negative ellipticities (Figure 2a, minima at 205 nm and 220 nm), characteristic of a helical population of conformers [21]. Addition of 40% trifluoroethanol (TFE) enhanced the helix signature. An extended β-sheet-like conformation was rapidly populated at the lower pH values required for nuclear magnetic resonance (NMR) experiments, however, as indicated by transition of the CD spectrum to that with a single minimum at 216 nm, positive ellipticity below 205 nm and an isodichroic point at 207 nm (Figure 2a). Furthermore, the addition of TFE did not increase helix content below pH 7. Although poor solubility of the synthetic propeptide (<500 μM) precluded the complete two-dimensional NMR analysis of $McbA_{1-26}$-COOH, a limited inspection of nuclear overhauser effect spectroscopy (NOESY) spectra acquired at pH 5.7 suggested a mixture of helix and extended conformations.

Subsequently, the carboxy-amidated derivative of the microcin B17 propeptide ($McbA_{1-26}$-$CONH_2$) was synthesized, with the expectation that masking the negative charge at the carboxyl terminus would minimize adverse interactions with the helix dipole and better mimic the covalent attachment of downstream residues (as in preproMccB17). Although the CD spectrum of $McbA_{1-26}$-$CONH_2$ in water at pH 5.7 indicated that the peptide was largely random coil with a small helical population, the net helicity increased significantly upon titration with only small amounts of TFE (Figure 2b). The addition of TFE caused two conformational effects. The first change was characterized by an increase in the absolute value of molar ellipticity at 222 nm that reached a plateau at ~20% TFE. The second effect was indicated by a similar increase in the absolute molar ellipticity at 208 nm that began at about 20% TFE and was mostly complete at 30% TFE. Both observations were consistent with increased stabilization of helical conformers by the addition of TFE. Unlike $McbA_{1-26}$-COOH, no drastic conformational change was observed for $McbA_{1-26}$-$CONH_2$ over the pH range 4.5–7.5, although a slight erosion of the TFE-stabilized helix conformation was observed above pH 6.5 (data not shown).

Determination of the solution structure of $McbA_{1-26}$-$CONH_2$

Guided by the CD analyses, one-dimensional ^1H spectra of the microcin leader peptide $McbA_{1-26}$-$CONH_2$ were examined in aqueous solution and with increasing concentrations of TFE to find optimal conditions for structure analysis. For a 1 mM sample in purely aqueous buffer at pH 5.7 and 25°C, proton resonances were spectrally dispersed except for the methyl protons (data not shown). In particular, the amide protons did not appear together as a

Figure 2

Preliminary conformational analysis of the microcin B17 propeptide. **(a)** Circular dichroism spectra of $McbA_{1-26}$-COOH acquired at different pH values. An overall conformational transition from α helix to β sheet is observed at pH <7.5. **(b)** Circular dichroism spectra of $McbA_{1-26}$-$CONH_2$ upon titration with TFE. Stabilization of a helical population of conformers is mostly complete upon the addition of 30% TFE.

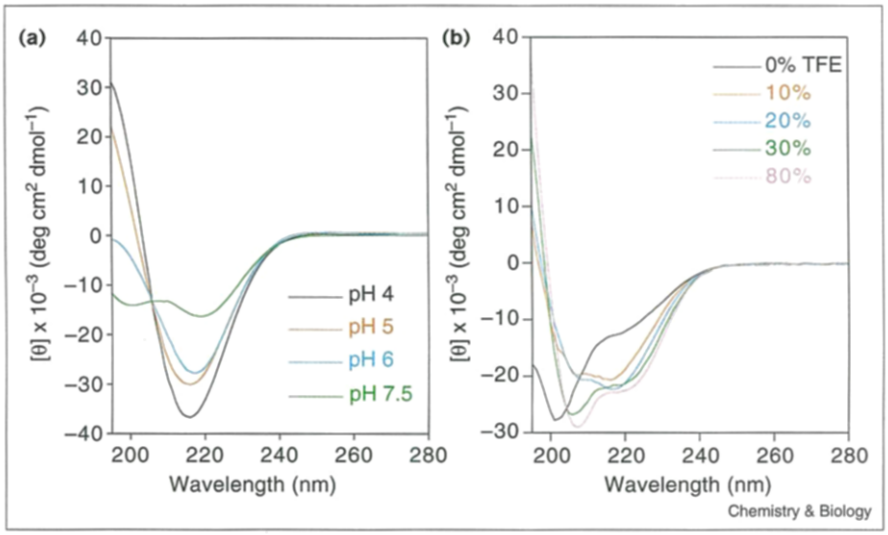

single broad resonance of overlapping peaks near 8.4 ppm, but were spread between 7.9 and 8.5 ppm. After recording two-dimensional NMR spectra for ~48 h, the sample formed a gel, however, and spectral quality was greatly diminished. In 20% TFE, an NMR spectrum was practically unobtainable, presumably because of the extensive line-broadening caused by intermediate-rate exchange between two or more conformers. Upon addition of TFE to 30% or above, however, the NMR spectrum was restored, but the resonance lines were slightly more disperse, especially in the methyl region, indicating a more ordered structure than that observed without TFE.

The improved solubility of $McbA_{1-26}$-$CONH_2$ in 40% TFE (>2 mM) allowed a detailed analysis of the peptide's solution structure. Two-dimensional NMR spectra of the peptide were recorded at 25°C in purely aqueous solution at pH 4.3 and in 40% TFE buffer at pH 5.7. The helical structure indicated by the CD studies was confirmed by the pattern of NOE cross-peaks for the peptide in 40% TFE (Figure 3). In the amide–amide proton region of the NOESY spectrum strong cross-peaks between sequential residues were observed for residues 6–22. Short-range and medium-range interactions were defined from the NOESY spectrum using the resonance assignments. Vicinal coupling constants between amide and Cα protons were measured from the observed splitting of amide proton cross-peaks in a resolution-enhanced NOESY spectrum [22]. For residues 5–19, the coupling constants were small (< 6 Hz), suggesting dihedral angles that were consistent with α-helix formation. The coupling constant data, amide–amide proton NOE interactions, and medium-range [Hα(i),Hβ(i+3)] NOE interactions defined a helical segment for the peptide between residues Ala5 and Arg21 (Figure 3). The absence of long-range NOE interactions between protons separated by four or more residues in the primary sequence indicated the lack of a compact tertiary structure and suggested that the peptide adopted an extended structure with the approximately central residues in a helical conformation. The helical structure was also supported by the observed chemical shifts of Cα protons for residues 5–20, that were shifted upfield by about 0.2 ppm relative to the 'standard' chemical shifts expected for an unstructured peptide [23,24].

The deviations from random coil values for Hα chemical shifts in 40% TFE mirrored the trends observed for the peptide in aqueous solution, but were slightly larger. The differences between the two solvent conditions were greatest at the immediate boundaries of the helix (residues 2–4 and residues 22–24) and near residue 12. Significantly, NOE data for the peptide in purely aqueous solution also showed sequential HN–HN cross-peaks for residues 5, 6 and 15–22. Other possible cross-peaks were masked by limited spectral dispersion and by poor signal-to-noise ratios as a result of limited sample solubility. Nevertheless, these results imply that 40% TFE stabilizes the structure inherent to the peptide in aqueous solution.

To determine the three-dimensional structure in detail for $McbA_{1-26}$-$CONH_2$ in 40% TFE, NOESY cross-peaks were converted into a set of distance restraints and calibrated using published methods [25,26]. From the coupling constant data, corresponding torsion angles were measured [27]. A set of 251 distance restraints and 23 torsion angles were used to generate 25 final structures using a combination of simulated annealing and distance geometry methods. The calculated structures were superimposed

Figure 3

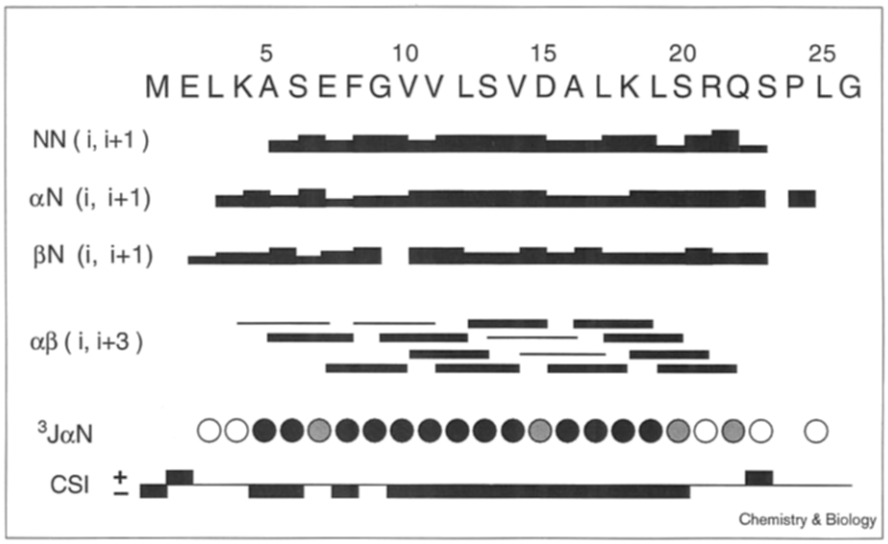

Summary of conformational data for the microcin B17 propeptide ($McbA_{1-26}$-$CONH_2$). NOE cross-peaks describing amide-to-amide contacts, Hα-amide contacts, Hβ-amide contacts and Hα(i)-Hβ(i+3) contacts are represented by the height of the filled-in bar corresponding to NOE intensity. The absence of a bar indicates that the NOE was not observed. Coupling constants to amide protons are indicated with filled circles for ^3J(HN,Hα) <6 Hz, open circles for ^3J(HN,Hα) >7 Hz, and shaded circles for ^3J(HN,Hα) between 6 and 7 Hz. The chemical shift index (CSI) is shown as positive if the difference between the observed Hα chemical shift and that for a random coil peptide was greater than + 0.1 ppm, and negative if it was less than − 0.1 ppm.

over residues 5–21 because these residues have uniformly well defined φ and ψ angles (Figure 4a). The pair-wise root mean square (rms) deviation for superimposed backbone atoms is 0.4 ± 0.2 Å; for all heavy atoms it is 1.0 ± 0.3 Å. PROCHECK analysis [28] showed that the backbone conformations of these residues were in the most favored region of the Ramachandran diagram (about 80%), or in the additional allowed region (about 20%), indicating a well-determined structure. The peptide adopts a helical conformation from Ala5 to Arg21 and has unstructured ends.

The propeptide helix is stabilized by two putative salt bridges (Lys4–Glu7 and Asp15–Lys18, Figure 4b) and helix dipole neutralization, in part by Glu2 and by Arg21. Three serine residues (Ser6, Ser13 and Ser20) are aligned on one face of the helix forming a polar surface (Figure 4b) that could be a possible site of interaction with the enzyme complex. In addition, a hydrophobic patch was found that comprises the well-ordered sidechains of Phe8, Leu12 and, to a lesser extent, Val11. These structural features were expected to be relevant for recognition by the MccB17 synthetase complex, and the relative importance of particular amino acid residues was tested by site-directed mutagenesis.

Site-directed mutagenesis of the microcin B17 propeptide

Structure–function effects of propeptide mutations would have been facilitated if $McbA_{1-26}$ could be tested in *trans* with downstream substrate fragments (eg. $McbA_{27-46}$). Although this two-peptide strategy employing effector and substrate fragments has been successfully used for measuring the activity of Vitamin K-dependent γ-carboxylase *in vitro* [29], preliminary experiments had indicated that it would not work for microcin B17 synthetase [8]. Indeed, in synthetase assays in which up to 100 μM $McbA_{1-26}$-COOH or $McbA_{1-26}$-$CONH_2$ was added in *trans* to downstream fragments ($McbA_{27-69}$, up to 2.5 mM, or α-amino-acetylated $McbA_{27-46}$, up to 1.2 mM), no heterocycle formation was detected (data not shown). Thus, the $McbA_{1-26}$ propeptide must be covalently connected to the downstream sequence for synthetase-mediated heterocycle formation. Furthermore, deletions in the polyglycine ($[Gly]_{10}$) linker connecting the propeptide to the first bis-heterocyclization site resulted in loss of turnover for analogs incorporating less than five glycine residues [30]. In the light of these experiments, the $McbA_{1-46}$ fragment incorporating the propeptide and the first bis-heterocyclization site (Gly39–Ser40–Cys41, Figure 1) was used as a minimal substrate for *in vitro* processing by the synthetase.

Site-directed mutagenesis (instead of chemical synthesis) was used to generate the 13 propeptide analogs described here. Individual residues in the MccB17 propeptide helix were varied to identify sidechains that are critical for recognition by the MccB17 synthetase. Mutagenesis of the propeptide segment was performed within a maltose-binding protein (MBP)–$McbA_{1-46}$ fusion protein framework reported earlier [30]. The relative efficiencies of 4,2-fused oxazole–thiazole formation in substrate analogs incorporating the different mutant propeptides were assessed by Western blots probed with antibodies raised against mature MccB17 that recognize heterocyclic polypeptide products but not preproMccB17 or fragments of preproMccB17 [6]. These polyclonal anti-MccB17 antibodies also recognize $McbA_{1-46}$ analogs containing only a single oxazole or thiazole heterocycle at positions 40 or 41 [30].

Figure 4

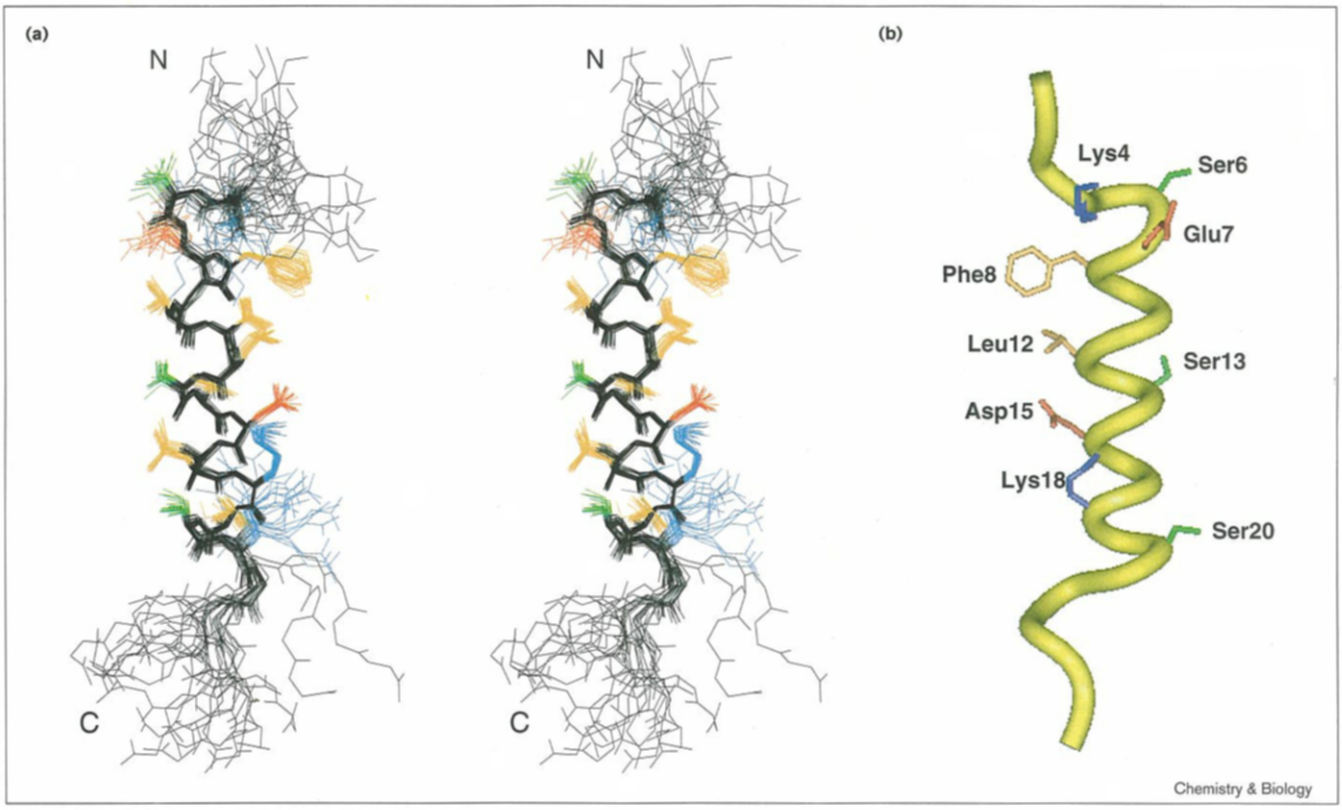

Solution structure of the microcin B17 propeptide. **(a)** Stereoview overlay of calculated backbone structures for the microcin leader peptide ($McbA_{1-26}$-$CONH_2$). The backbone atoms for 25 structures were superimposed for residues 5–21. The pair-wise rms deviation for these ordered residues was 0.4 ± 0.2 Å. Sidechains were well ordered for residues 5–20. The sidechains of acidic residues are red, those of basic residues are blue, serine residues are green and hydrophobic residues are orange. For clarity, the sidechains of residues 1–3 and 22–26 have been omitted. **(b)** Ribbon diagram of the microcin B17 propeptide helix highlighting key structural features. Two putative salt bridges (Lys4–Glu7 and Asp15–Lys18) stabilize the helix. Key hydrophobic residues (Phe8 and Leu12) on the nonpolar face are recognized by MccB17 synthetase. An array of serine residues (Ser6, Ser13 and Ser20) span the moderately polar face of the helix.

Mutagenesis of the polar face of the propeptide helix

To determine whether the moderately polar face comprising residues Ser6, Ser13 and Ser20 was important for interaction with the McbB,C,D synthetase, each serine residue was individually replaced by alanine in mutants S6A, S13A and S20A. The MBP–$McbA_{1-46}$ mutants were purified by affinity chromatography on an amylose column. Western blots for incubation of these substrate analogs with affinity-purified calmodulin-binding peptide (CBP)-tagged MccB17 synthetase are presented in Figure 5, along with the wild-type MBP–$McbA_{1-46}$ (WT) results for comparison. No appreciable difference in the efficiency of heterocycle-containing product formation was observed for any particular mutant protein, indicating that the serine residues (and the polar helix face) were not essential for synthetase recognition.

Role of the putative salt bridges in propeptide recognition

The stabilization of α helices by salt bridges (electrostatic and hydrogen bond interactions between charged residues of opposite polarity), which lock the folded conformation, is well documented [31–33]. Two salt bridges (Lys4–Glu7 and Asp15–Lys18) are suggested by the

Figure 5

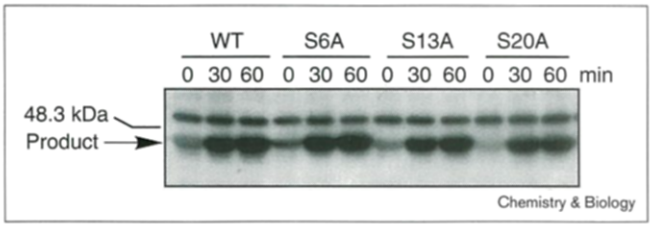

Protein immunoblots for incubations of MBP–$McbA_{1-46}$ (WT), and mutants S6A, S13A and S20A with CBP-tagged MccB17 synthetase. Comparable time-dependent bis-heterocyclic product formation is observed in each system. The ~67 kDa band in each lane arises from nonspecific recognition of a contaminant in the synthetase preparation by the polyclonal anti-MccB17 antibodies used in the Western assay.

Figure 6

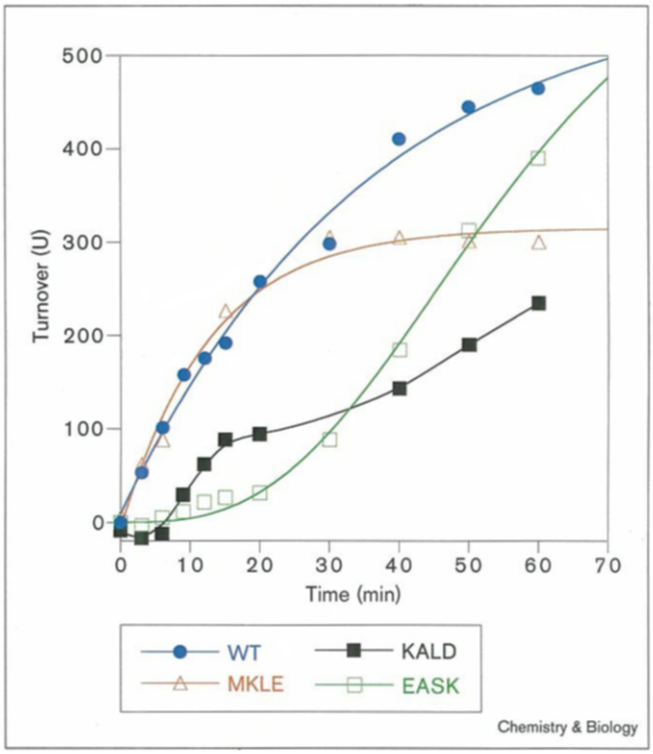

Effects of electrostatic perturbations on heterocyclization of wild-type and mutant propeptides. Relative kinetics of processing by MccB17 synthetase for MBP–McbA$_{1-46}$ (WT), and the propeptide mutants MKLE, KALD and EASK. U, arbitrary units.

Figure 7

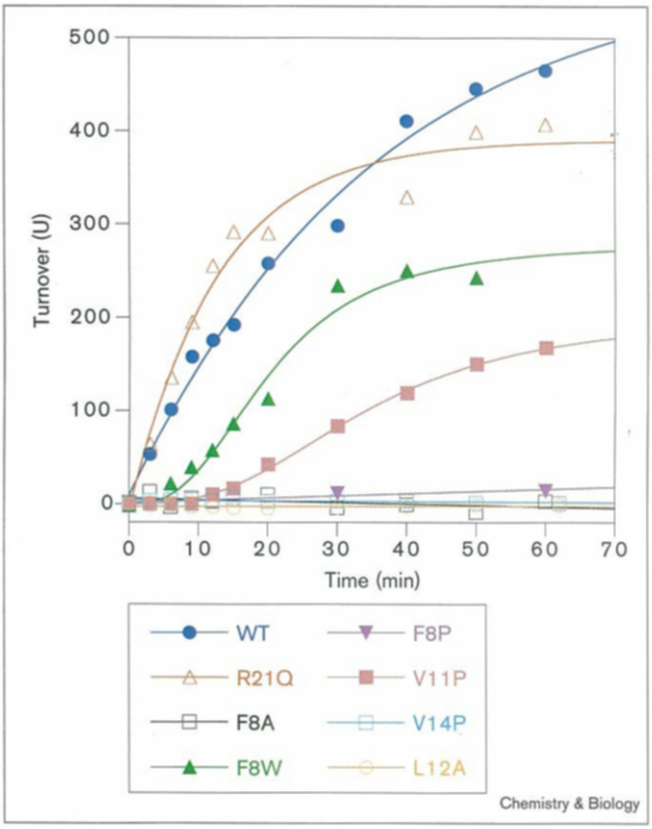

Relative kinetics of heterocyclization for MBP–McbA$_{1-46}$ (WT) and different propeptide mutants. U, arbitrary units.

solution structure of the propeptide helix. As Lys4 is proximal to Glu2, an electrostatic interaction between the sidechains of these residues is also possible. Mutagenesis of these positions was therefore performed to evaluate the importance of electrostatic interactions in the propeptide helix. Each putative salt-bridge pair was inverted in the propeptide primary sequence to assess the impact of a reversed charge polarity on synthetase binding and substrate turnover. Thus, MBP–McbA$_{1-46}$ proteins MKLE, EASK and KALD incorporate propeptides with the putative 'reversed' salt bridges Lys2–Glu4, Glu4–Lys7 and Lys15–Asp18, respectively. The relative kinetics of processing for these substrate analogs by the synthetase are illustrated in Figure 6. Interchanging Lys4 and Glu2 in mutant MKLE did not appreciably perturb the initial rate of turnover relative to WT. In contrast, the EASK and KALD mutants had a considerable lag phase (5–15 min), and the KALD protein was processed approximately ninefold slower than WT. The unusual kinetics observed with the EASK and KALD mutants may result from an initial weak recognition of the mutant propeptides leading to slow formation of the first heterocycle and positive cooperativity precipitating rapid formation of the second heterocycle.

Identification of propeptide residues essential for synthetase recognition

The Arg21→Asn (R21Q), Phe8→Ala (F8A), and Leu12→Ala (L12A) propeptide mutants were investigated next in a search for individual charged or hydrophobic residues that might serve as key recognition features for the MccB17 synthetase. As shown in Figure 7, R21Q was comparable to the wild-type substrate in turnover efficiency. In contrast, no heterocycle formation was detected in Western blots with the F8A and L12A analogs, thus implicating Phe8 and Leu12 as important residues in propeptide recognition. To further elucidate the sidechain requirements in this region, the Phe8→Trp (F8W) mutant was evaluated. A prerequisite for aromatic/hydrophobic residues at position 8 was confirmed by the turnover of F8W, albeit at a rate fourfold slower than that of WT.

The complete absence of turnover observed with the F8A and L12A substrate analogs could be a result of an altered (nonproductive) binding mode of the mutant propeptides, or could arise from a lack of synthetase recognition of the modified propeptides. To distinguish between these two possibilities, the binding competence of one of these

Figure 8

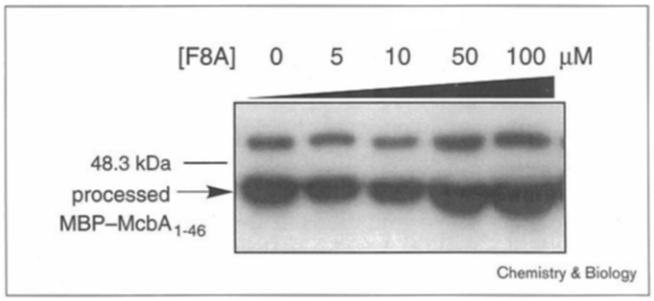

Protein immunoblot for assaying the inhibitory capacity of propeptide mutant F8A in the turnover of MBP–$McbA_{1-46}$ by MccB17 synthetase. Less than 10% inhibition in the turnover of substrate (10 μM) is observed upon the addition of up to 100 μM F8A.

proteins (F8A) was evaluated in a competition assay with WT. Figure 8 shows the Western blot for a 10 min incubation of WT substrate (10 μM MBP–$McbA_{1-46}$) with synthetase and increasing concentrations of F8A (0–100 μM). No significant inhibition in the turnover of MBP–$McbA_{1-46}$ was detected upon titration with F8A, even when F8A was in large excess (<10% inhibition at 100 μM F8A). These data imply a decrease in substrate-binding affinity of at least 200-fold upon substitution of Phe8 (or by inference, Leu12). Thus, the failure of the F8A mutant as both a substrate and an inhibitor reflects the inability of MccB17 synthetase to recognize and bind propeptides lacking hydrophobic residues at positions 8 or 12.

Distortion of helical structure disrupts substrate recognition

To establish further the relevance of the propeptide helix conformation to its biological role of substrate recognition, the effect of incorporating a 'helix breaker' (proline) was examined at three different positions in the helix. Residues Phe8, Val11 and Val14 were each replaced by proline in mutants F8P, V11P and V14P, respectively. The turnover kinetics for each protein are shown in Figure 7. Substrate analog V11P was processed only slowly, with a considerable lag phase. Furthermore, proteins F8P and V14P were completely inactive as substrates. As Val11/14→Ala mutations in full length McbA do not affect antibiotic efficacy in bioassays with MccB17-sensitive strains [34], the disruption in substrate turnover for mutants V11P and V14P must arise from the conformational consequences of introducing proline into the propeptide helix. Similarly, although the Phe8→Pro substitution in mutant F8P does not drastically alter the hydropathic profile of the propeptide sequence, the resulting helix distortion is sufficient to abolish substrate turnover completely.

Discussion

Many post-translationally modified polypeptides arise from precursors incorporating an amino-terminal leader peptide. The leader peptide often contains the determinants for recognition by the modifying enzyme or enzyme complex, and is removed concomitant with formation or secretion of the mature product. Propeptide recognition elements are observed in blood coagulation proteins such as prothrombin and Factor IX, which incorporate γ-carboxylase recognition sequences [16], and in lantibiotics secreted by gram-positive bacteria, in which leader sequences direct the carboxy-terminal domains for enzymatic modifications such as dehydration and thioether ring formation [35]. Similarly, MccB17, a DNA gyrase inhibitor [36] secreted in stationary phase by several strains of *Escherichia coli* and the object of this study, arises from the post-translational heterocyclization of a 69 amino acid precursor polypeptide (McbA) incorporating a 26 residue leader sequence that forms the recognition determinant for microcin B17 synthetase [8].

The three-dimensional structures of leader peptides have typically been studied in the absence of their target enzymes [37–39]. The enzymes that recognize the leader sequences are either membrane bound or contain multiple subunits, and have therefore been unavailable in quantities sufficient for biophysical characterization in the form of complexes. The leader sequences adopt a mostly unstructured conformation in aqueous solution (in the absence of partner protein), but readily form α-helical segments in the presence of TFE. TFE usually does not induce helical structure, rather it stabilizes helices in regions with an intrinsic α-helical propensity [40,41]. The leader sequence of prothrombin [39] and the homologous region from Factor IX [37] form an amphipathic helix in 40% TFE and the amino acid residues important for recognition (as determined by mutagenesis) are located on a hydrophobic patch on a face of the helix near the amino terminus. Similarly, the leader sequence for the precursor form of the lantibiotic nisin, although mostly unstructured in aqueous solution [38], readily formed an amphipathic helix in the presence of TFE.

In this work, the microcin B17 leader peptide has been observed to form an α helix (residues 5–21) that was stabilized by TFE in aqueous solution. The propeptide is separated from the first heterocyclization site (Gly39–Ser40–Cys41) by a polyglycine stretch of 10 residues that is unlikely to be structured. The leader sequence and the modified portion of the MccB17 substrate thus appear to be two independent folding units. A similar phenomenon has been observed for pronisin; the conformation of the nisin portion is unchanged by the presence of the leader sequence [38]. Furthermore, the MccB17 propeptide fragment ($McbA_{1-26}$) inhibits synthetase-mediated bis-heterocyclization of $McbA_{1-46}$ with an IC_{50} value comparable to the K_m of substrate [8]. Thus, the recognition and modification elements of preMccB17 precursor appear to be separable functions, although the

Figure 9

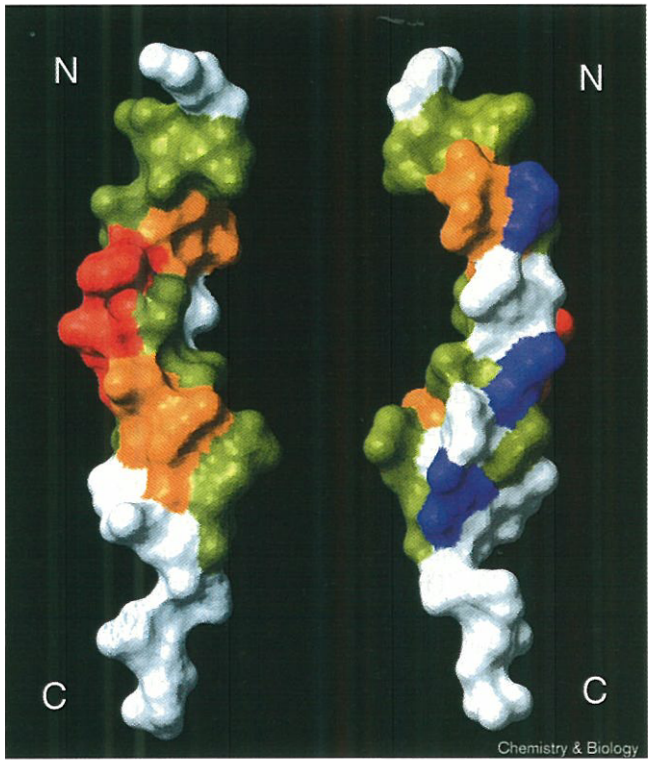

Mutagenesis results mapped onto the solvent accessible surface of the propeptide helix. Diametrically opposite views are shown. Residues that can be substituted without adversely affecting synthetase-mediated heterocyclization or antibiotic efficacy are yellow. Also included in this category are the serine residues highlighted in blue on the right (Ser6, Ser13, Ser20). Reversals of putative salt bridges that decrease turnover or bioactivity are highlighted in orange. Hydrophobic residues essential for synthetase recognition are red (Phe8 and Leu12). A probable domain of propeptide interaction with the synthetase complex emerges in the view on the left (orange/red). Residues not included in this analysis are colored white.

polyglycine linker is essential to achieve a correct register between the α-helical propeptide and cyclizable serine and cysteine residues [30].

The structure–function data reported here for 13 propeptide mutants in the context of $McbA_{1-46}$ substrate analogs can be interpreted on the basis of the solution structure obtained for $McbA_{1-26}$. Perturbations in synthetase-mediated turnover of individual MBP–$McbA_{1-46}$ propeptide mutants were mapped onto the three-dimensional structure of the propeptide fragment to produce the model depicted in Figure 9. Bioactivity data [34] for antibiotic efficacy of a complementary set of mutations in the leader sequence of McbA were also included in the analysis (Figure 10). Those data were obtained by comparing zones of growth inhibition on lawns of MccB17-sensitive indicator cells exposed to cell extracts containing the mature McbA mutants, and would score mutations that affected not only post-translational heterocyclization, but also subsequent proteolytic cleavage of the propeptide and secretion of mature MccB17. As shown in Figure 9, mutations that adversely affect substrate processing are clustered on a single face of the propeptide helix, spanning residues Lys4, Glu7, Phe8, Leu12, Asp15 and Lys18. This face probably represents the domain that interacts with the synthetase complex during the initial recognition of the 69 amino acid McbA substrate by the McbB,C,D synthetase complex.

The strategy of recruiting hydrophobic sidechains spaced four residues apart in the leader (Phe8, Leu12) for recognition by modifying enzymes may be a general one. The precursor propeptide for trifolitoxin [42], a rhizobial peptide that contains a thiazoline heterocycle derived from the post-translational modification of Cys [43], shows limited homology to $McbA_{1-26}$, but has an equivalent pattern of hydrophobic residues in the putative helical prosequence (Ile16, Phe20 and Leu24). These residues may therefore provide most of the recognition determinants for TfxB, -D, and -F, the cognate enzymes for post-translational modification [42]. Although the serine residues in the microcin leader are not important for substrate recognition by the heterocyclizing synthetase, the moderately polar face spanned by these residues might constitute a second recognition surface for interaction with the cell membrane, and target preproMccB17 for secretion by the membrane-bound

Figure 10

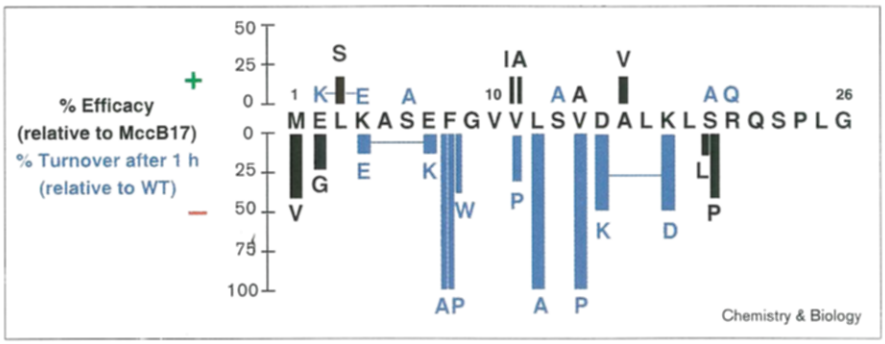

Summary of structure–activity relationships for the MccB17 propeptide. Bioassay data [34] are indicated in black. Mutagenesis results from this study are presented in blue. Pair-wise mutations are connected by a horizontal line. The bioassay data for Met1 and Glu2 mutants were excluded in the map shown in Figure 9, because antibiotic efficacy perturbations resulting from substitutions at these positions were attributed to decreases in translational efficiency of the mutant *mcbA* structural gene.

Figure 11

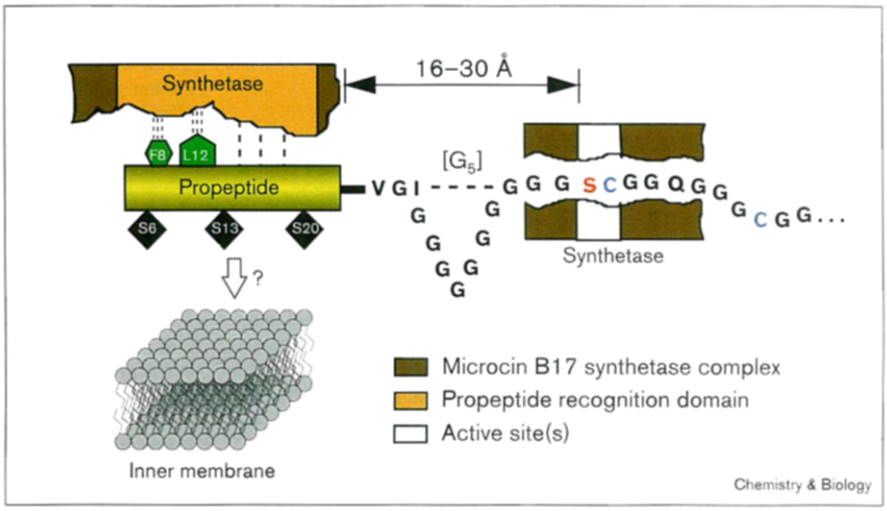

Proposed model for the substrate–synthetase interaction in the microcin B17 system. The amino-terminal propeptide sequence (yellow) is initially recognized by a specific domain (orange) in the MccB17 synthetase complex. Residues Phe8 and Leu12 (green) play key roles in this recognition event. The polyglycine linker acts as a spacer and sets the register to allow heterocyclization of specific downstream serine (red) and cysteine (blue) residues at a spatially distinct active site (white) in the synthetase. The shortest functional linker in this regard comprises five glycine residues [G_5] [30], allowing an estimate of the separation between the propeptide recognition domain and the heterocyclization active site(s). The moderately polar propeptide face includes an array of serine residues that might interact with the inner membrane and target the processed antibiotic for secretion by the dedicated MccB17 transporter (McbE,F), concomitant with cleavage of the propeptide leader sequence.

dedicated transporter (McbE,F). A similar array of serine residues (Ser260, Ser271 and Ser282) has been observed in the amphipathic helical domain of the amphitropic regulatory enzyme CTP:phosphocholine cytidyltransferase that interacts with the lipid bilayer [44]. As in this system, Ser6, Ser13 and Ser20 in the MccB17 propeptide might serve to limit the hydrophobicity of the membrane interaction face and modulate the selectivity of lipid binding.

The polyheterocyclization achieved by interaction of McbA as substrate with McbB,C,D as catalysts is remarkable both in terms of the chemical reactions and positioning of the residues that determines which serine and cysteine residues get cyclized. Together with mutagenesis results at the Gly39–Ser40–Cys41 bis-heterocyclization site of McbA [30], the studies presented here on the MccB17 propeptide suggest the two-site interaction model presented in Figure 11 for protein–protein recognition in the microcin B17 system.

Significance

The DNA-gyrase-targeting activity of the *Escherichia coli* peptide antibiotic microcin B17 (MccB17) depends on the unusual post-translational modification of six glycine, four serine and four cysteine residues (spanning residues 39–67 of the McbA structural gene product) to four oxazole and four thiazole heterocycles. The heterocyclization process completely depends on upstream residues ($McbA_{1-26}$) that serve as the high affinity recognition element for the processing McbB,C,D enzyme complex. The solution structure of the propeptide $McbA_{1-26}$-$CONH_2$ reveals an amphipathic α helix spanning residues 5–21. This analysis, using nuclear magnetic resonance, facilitated site-directed mutagenesis of propeptide residues within a competent substrate fragment ($McbA_{1-46}$). The structural and mutagenesis data were subsequently combined to map the initial interaction surface of the McbA substrate with the McbB,C,D synthetase complex. The hydrophobic patch, containing Phe8 and Leu12, in the MccB17 propeptide is a key binding determinant. This work sets the stage for evaluating the effects of McbA propeptide mutations on interactions with the transport (McbE,F) and immunity (McbG) proteins of the MccB17 operon, which might affect antibiotic secretion and efficacy.

Materials and methods

CBP-tagged microcin B17 synthetase incorporating the McbB subunit affinity-labeled with calmodulin-binding peptide [45,46] was overexpressed and purified as reported earlier [30]. Polyclonal rabbit anti-MccB17 antibodies were generated by East Acres Biologicals. Horseradish peroxidase (HRP)-conjugated goat anti-rabbit IgG (H+L) polyclonal antibody was purchased from Pierce. Plasmid pMSS10 encoding the MBP–$McbA_{1-46}$ fusion protein under control of the T7 promoter, and plasmid pIADL14 encoding MBP–VanX fusion protein have been described elsewhere [30,47]. Oligonucleotide primers were obtained from Integrated DNA Technologies, Gene Link, or Biosource International.

Peptide synthesis

Synthetic polypeptides $McbA_{1-26}$-COOH and $McbA_{1-26}$-$CONH_2$ were synthesized on an automated peptide synthesizer at the Howard Hughes Biopolymer Facility, Harvard Medical School using solid phase Fmoc-based peptide synthesis [48]. Each polypeptide was purified by C_{18} reversed phase high performance liquid chromatography (HPLC) and its identity was confirmed using matrix-assisted laser desorption ionization (MALDI) mass spectrometry.

Circular dichroism spectroscopy

CD spectra were recorded with an Aviv Model 62DS CD spectrophotometer. Spectra were baseline corrected and noise-reduced using

Aviv system software. The ellipticity (θ_{obs}) of polypeptide solutions (20–50 μM) in 10 mM phosphate or acetate buffer was measured at 25°C over the range 190–280 nm using four scans and an averaging time of 1 s in a 0.1 cm cuvette. The CD data are reported as mean residue ellipticity ([θ], in deg.cm^2.dmol^{-1}).

NMR spectroscopy and structure calculation

Lyophilized peptide (2 or 4 mM) was solubilized in a buffer containing 100 mM NaCl, 10 mM Na_2HPO_4, and 10 mM NaH_2PO_4, pH 4.3 or in a buffer containing 40% TFE, 100 mM NaCl, 10 mM Na_2HPO_4, and 10 mM NaH_2PO_4, pH* 5.7. Samples also contained 10% D_2O for the deuterium lock signal. For 4 mM samples in D_2O, the peptide was lyophilized and then redissolved in 99.96% D_2O and 40% TFE, pH 5.7. Spectra were collected at 15°C and 25°C, on a Bruker AMX-500 spectrometer with a proton frequency of 500.14 MHz. The carrier frequency was set on the water resonance, which was suppressed using presaturation. Two-dimensional NOESY, total correlation spectroscopy (TOCSY), and double quantum filtered correlation spectroscopy (DQF-COSY) spectra [49] were collected in H_2O, and a NOESY spectrum was obtained in D_2O to uncover proton signals buried underneath the water resonance. NOESY spectra were obtained at two different temperatures to separate overlapping resonances or to shift resonances bleached out by saturation of the water resonance under one set of conditions but not the other. NOESY spectra were acquired with mixing times of 250 ms for the sample at 25°C and 400 ms at 15°C. A total of 4096 real data points was acquired in t_2 with 512 time-proportional phase increments in t_1, a spectral width of 6024 Hz, 144 summed scans, and a relaxation delay of 1.2 s between scans. Spectra were multiplied with sine-bell window functions shifted by 45° in t_2 (applied over 1024 points) and 60° in t_1 (applied over 512 points) and zero filled to a 2048 × 1024 (real) matrix using Bruker NMR processing software. NOESY cross-peak intensities were converted into distance restraints and calibrated against internal standards involving amide proton-to-Hα distances [25,26]. A TOCSY spectrum was recorded and processed using parameters identical to the NOESY experiment, except with a mixing time of 46 ms, 96 scans, and using an MLEV-17 mixing sequence [49]. A DQF-COSY spectrum was collected with 2048 real t_2 points using a spectral width of 6024 Hz, 768 t_1 TPPI increments, and a relaxation delay of 1.3 s between scans. Spectra were apodized with sine bells shifted by 30° in t_2 and by 45° in t_1 and zero-filled to a 2048 × 1024 (real) matrix.

Protons were assigned to their resonance positions following standard homonuclear methods [27]. Briefly, intraresidue connectivities were established via TOCSY and DQF-COSY experiments followed by a search for sequential (HN(i),HN(i+1)), (Hα(i),HN(i+1)), and (Hβ(i+1),HN(i+1)) cross-peaks in the NOESY spectrum. Starting points for assignment were identification of the amino acid spin systems for the single phenylalanine residue Phe8, the single aspartate residue Asp15, and the single arginine residue Arg21.

NOESY cross-peak intensities were converted into distances and calibrated using published methods [25,26]. Comparison of NOESY spectra collected at two mixing times was used to control for spin diffusion effects. Non-stereospecifically assigned atoms were treated as pseudoatoms and given correction distances [27]. The vicinal coupling constants, ^{3}J(HN,Hα), were measured from the splitting of cross-peaks in the HN dimension in a NOESY spectrum that was resolution-enhanced during processing using a squared sine-bell window function shifted by 30° applied over 2048 (real) points in t_2 [22]. Only residues with ^{3}J(HN,Hα) < 6 Hz were used for structure determination (15 in total). For some residues, φ angle constraints were limited to the negative range by referring to both the size of the coupling constants and intensity of NOE cross-peaks for intraresidue *dN(i,i)*, and sequential *dN(i,i+1)* and *dNN(i,i+1)* connectivities [50]. χ1 torsion angles and β-methylene proton stereospecific assignments were determined from a measurement of ^{3}J(Hα,Hβ), and a comparison of the Hβ-HN and Hα-Hβ cross-peak intensities in the NOESY spectra for each stereospecific β proton of AMX residues. ^{3}J(Hα,Hβ) (11 in total) were measured from the splitting in the Hα dimension of cross-peaks from a NOESY spectrum collected in D_2O solution. χ_1 Torsion angles for valine residues were obtained for a measurement of ^{3}J(Hα,Hβ) and an analysis of the Hα-Hβ NOE cross-peak shapes [51].

Structure determination used a set of 251 distance restraints and 26 torsion angles that were entered into the DGII program of InsightII (Biosym Technologies, San Diego, CA). A combination of distance geometry and simulated annealing methods generated 30 structures using previously published methods [52], of which 29 converged, and 25 structures were randomly chosen and used for further analysis. They were superimposed using the backbone atoms over well defined φ and ψ angles [25]. The average rms deviation values and PROCHECK analysis [28] reflected the quality of the structures determined.

Site-directed mutagenesis of MBP–McbA$_{1-46}$

The 1371 base pair *XbaI-XhoI* fragment from pMSS10 was subcloned into the 5192 base pair vector backbone obtained from *XbaI/XhoI* digestion of plasmid pIADL14 to generate plasmid pMSS46 (microcin synthetase substrate) using recombinant DNA techniques described elsewhere [53]. Plasmid pMSS46 is identical to plasmid pMSS10 except for the presence of a *SmaI* site in the former.

Propeptide mutants S6A, S13A, and S20A were generated by Unique Site Elimination (USE) mutagenesis [54] of plasmid pMSS10 as described earlier [30], with the selection primer 5′-CCCATACAATCGGT-AGATTGTCGCAC-3′ (for elimination of the *ClaI* site), and the following mutagenic primers: S6A, 5′-GAATTAAAAGCGGCTGAATTTGGTGT-3′; S13A, 5′-GGTGTAGTTTTGGCCGTTGATGCTCTT-3′; S20A, 5′-GCT-CTTA-AATTAGCACGCCAGTCTC-3′. Propeptide mutant V14P was constructed by USE mutagenesis of pMSS46 with the mutagenic primer 5′-GGTGTAGTTTTGTC-CCCTGATGCTCTTAAATTATCACGC-3′.

Propeptide mutants MKLE, EASK, F8A, F8W, F8P, V11P and L12A were generated by PCR mutagenesis of plasmid pMSS10 (MKLE, F8A, F8W, V11P) or pMSS46 (EASK, F8P, L12A) using the *BamHI* and *DraIII* sites, as described elsewhere [30]. The reverse primer was 5′-CGTCTATCAGGGCGATGGCCCACTACG-3′ and the forward primers were: MKLE, 5′-ACGAGGATCCATGAAATTAGAAGCGAGTG-AATTTGG-3′; EASK, 5′-ACGAGGATCCATGGAATTAGAAGCGAGT-AAATTTGGTGTAG-3′; F8A, 5′-ACGAGGATCCATGGAATTAAAAG-CGAGTGAAGCGGGTGTAGTTTTGTCCG-3′; F8W, 5′-ACGAGGAT-CCATGGAATTAAAAGCGAGTGAATGGGGTGTAGTTTTGTCCG-3′; F8P, 5′-ACGAGGATCCATGGAATTAAAAGCGAGTGAACCGGGT-GTAG-3′; V11P, 5′-ACGAGGATCCATGGAATTAAAAGCGAGT-GAATTTGGTGTACCG-TTGTCCGTTG-3′; L12A, 5′-ACGAGGATC-CATGGAATTAAAAGCGAGTGAATTTG-GTGTAGTTGCGTCCGTT-GATGC-3′. Mutant propeptides KALD and R21Q were constructed by PCR mutagenesis of pMSS10 using the *BsiWI* and *AvrII* sites, the forward primer 5′-GGATGCCGTACGTTACAACGGCAAGCTG-3′, and the reverse primers: KALD, 5′-AACACCTAGGGGAGACTGGCGT-GATAAATCAAGAGCTTTAACGGA-CAAAAC-3′; R21Q, 5′-CCAAC-ACCTAGGGGAGACTGCTGTGATAATTTAAGAG-CATCAACG-3′.

Overexpression of propeptide mutants and Western blot assays

The MBP–McbA$_{1-46}$ fusion proteins were expressed in BL21(DE3) cells cultures in LB media containing kanamycin (50 μg per ml). Cultures were induced with 1 mM IPTG in mid-log phase and harvested 3 h later. Resuspended cells were lysed twice in a French press and purified using a single step affinity chromatography on an amylose column as described elsewhere [30]. Purified MBP–McbA$_{1-46}$ fusion proteins were assayed as substrates for CBP-tagged MccB17 synthetase (CBP-McbBCD) using an *in vitro* Western blot assay described earlier [30].

Accession numbers

The NMR restraints and coordinates for the microcin leader peptide (accession numbers: r2mlpmr and 2mlp) have been deposited with the Protein Data Bank, Brookhaven National Laboratory, Upton, New York, 11923, USA, from whom copies can be obtained.

Supplementary material

Supplementary material published with this paper on the internet includes: two figures of NMR data and two tables of proton NMR resonance assignments for the microcin B17 leader peptide ($McbA_{1-26}$-$CONH_2$) in 40% TFE and in purely aqueous solution.

Acknowledgements

This research was supported by NIH Grant GM 20011 to C.T.W. and by NIH grant HL 42443 to J.D.B. R.S.R. is a Parke-Davis Fellow of the Life Sciences Research Foundation. The NMR spectrometer was acquired with a grant (RR06282) from the NIH. We thank Jill Milne for critical reading of the manuscript.

References

1. Kolter, R. & Moreno, F. (1992). Genetics of ribosomally synthesized peptide antibiotics. *Annu. Rev. Microbiol.*, 141-163.
2. Jack, R.W., Tagg, J.R. & Ray, B. (1997). Bacteriocins of gram-positive bacteria. *Microbiol. Rev.* **59**, 171-200.
3. Moreno, F., San Millán, J.L., Hernández-Chico, C. & Kolter, R. (1995). Microcins. In *Genetics and Biochemistry of Antibiotic Production.* (Vining, C.L. & Stuttard, C., eds), pp. 307-321, Butterworth-Heinemann, Boston.
4. Davagnino, J., Herrero, M., Furlong, D., Moreno, F. & Kolter, R. (1986). The DNA replication inhibitor microcin B17 is a forty-three-amino-acid protein containing sixty percent glycine. *Proteins: Struct. Funct. Genet.* **1**, 230-238.
5. Bayer, A., Freund, S., Nicholson, G. & Jung, G. (1993). Posttranslational backbone modifications in the ribosomal biosynthesis of the glycine-rich antibiotic microcin B17. *Angew. Chem. Int. Ed. Engl.* **32**, 1336-1339.
6. Yorgey, P., Davagnino, J. & Kolter, R. (1993). The maturation pathway of microcin B17, a peptide inhibitor of DNA gyrase. *Mol. Microbiol.* **9**, 897-905.
7. Yorgey, P., *et al.*, & Kolter, R. (1994). Posttranslational modifications in microcin B17 define an additional class of DNA gyrase inhibitor. *Proc. Natl Acad. Sci. USA* **91**, 4519-4523.
8. Li, Y.-M., Milne, J.C., Madison, L.L., Kolter, R. & Walsh, C.T. (1996). From peptide precursors to oxazole and thiazole-containing peptide antibiotics: Microcin B17 synthase. *Science* **274**, 1188-1193.
9. Garrido, M.C., Herrero, M., Kolter, R. & Moreno, F. (1988). The export of the DNA replication inhibitor microcin B17 provides immunity for the host cell. *EMBO J.* **7**, 1853-1862.
10. Fath, M.J. & Kolter, R. (1993). ABC transporters: Bacterial exporters. *Microbiol. Rev.* **57**, 995-1017.
11. San Millán, J.L., Kolter, R. & Moreno, F. (1985). Cloning and mapping of the genetic determinants for microcin-B17. *J. Bacteriol.* **163**, 275-281.
12. San Millán, J.L., Kolter, R. & Moreno, F. (1985). Plasmid genes required for microcin B-17 production. *J. Bacteriol.* **163**, 1016-1020.
13. den Blaauwen, T. & Driessen, A.J.M. (1996). Sec-dependent preprotein translocation in bacteria. *Arch. Microbiol.* **165**, 1-8.
14. Madison, L.L., Vivas, I.E., Li, Y.-M., Walsh, C.T. & Kolter, R. (1997). The leader peptide is essential for the post-translational modification of the DNA gyrase inhibitor microcin B17. *Mol. Microbiol.* **23**, 161-168.
15. Hubbard, B.R., Jacobs, M., Ulrich, M.M.W., Walsh, C., Furie, B. & Furie, B.C. (1989). Vitamin-K-dependent carboxylation - in vitro modification of synthetic peptides containing the γ-carboxylation recognition site. *J. Biol. Chem.* **264**, 14145-14150.
16. Huber, P., *et al.*, & Furie, B. (1990). Identification of amino acids in the γ-carboxylation recognition site on the propeptide of prothrombin. *J. Biol. Chem.* **265**, 12467-12473.
17. Furie, B. & Furie, B.C. (1988). The molecular basis of blood-coagulation. *Cell* **53**, 505-518.
18. de Vos, W.M., Kuipers, O.P., van der Meer, J.R. & Siezen, R.J. (1995). Maturation pathway of nisin and other lantibiotics: Post translationally modified antimicrobial peptides exported by gram-positive bacteria. *Mol. Microbiol.* **17**, 427-437.
19. van Belkum, M.J., Worobo, R.W. & Stiles, M.E. (1997). Double-glycine-type leader peptides direct secretion of bacteriocins by ABC transporters: Colicin V secretion in *lactococcus lactis*. *Mol. Microbiol.* **23**, 1293-1301.
20. Chou, P.Y. & Fasman, G.D. (1978). Prediction of the secondary structure of proteins from their amino acid sequence. *Adv. Enzymol.* **47**, 45-148.
21. Woody, R.W. (1996). Theory of circular dichroism of proteins. In *Circular Dichroism and the Conformational Analysis of Biomolecules.* (Fasman, G.D., ed.), pp. 25-67, Plenum Press, New York.
22. Szyperski, T., Güntert, P., Otting, G. & Wüthrich, K. (1992). Determination of scalar coupling constant by inverse fourier transform of in-phase multiplets. *J. Magn. Res.* **99**, 552-560.
23. Merutka, G., Dyson, H.J. & Wright, P.E. (1995). 'Random coil' ^1H chemical shifts obtained as a function of temperature and trifluoroethanol concentration for the peptide series GGXGG. *J. Biomol. NMR* **5**, 14-24.
24. Wishart, D.S., Sykes, B.D. & Richards, F.M. (1991). Relationship between nuclear magnetic resonance chemical shift and protein secondary structure. *J. Mol. Biol.* **222**, 311-333.
25. Hyberts, S.G., Goldberg, M.S., Havel, T.F. & Wagner, G. (1992). The solution structure of eglin C based on measurements of many NOEs and coupling constants and its comparison with X-ray structures. *Protein Sci.* **1**, 736-751.
26. Detlefsen, D.J., Thanabal, V., Pecoraro, V.L. & Wagner, G. (1991). Solution structure of Fe(II) cytochrome *c*551 from *Pseudomonas aeruginosa* as determined by two-dimensional ^1H NMR. *Biochemistry* **30**, 9040-9046.
27. Wüthrich, K. (1986). *NMR of Proteins and Nucleic Acids.* Wiley, New York.
28. Laskowski, R.A., Macarthur, M.W., Moss, D.S. & Thornton, J.M. (1993). PROCHECK: A program to check the stereochemical quality of protein structures. *J. Appl. Crystallogr.* **26**, 283-291.
29. Ulrich, M.M.W., Furie, B., Jacobs, M.R., Vermeer, C. & Furie, B.C. (1988). Vitamin K-dependent carboxylation: a synthetic peptide based upon the γ-carboxylation recognition site sequence of the prothrombin propeptide is an active substrate for the carboxylase *in vitro*. *J. Biol. Chem.* **263**, 9697-9702.
30. Sinha Roy, R., Belshaw, P.J. & Walsh, C.T. (1998). Mutational analysis of posttranslational heterocycle biosynthesis in the gyrase inhibitor microcin B17: Distance dependence from propeptide and tolerance for substitution in a GSCG cyclizable sequence. *Biochemistry* **37**, 4125-4136.
31. Marqusee, S. & Baldwin, R.L. (1987). Helix stabilization by Glu^-... Lys^+ salt bridges in short peptides of de novo design. *Proc. Natl Acad. Sci. USA* **84**, 8898-8902.
32. Lyu, P.C., Marky, L.A. & Kallenbach, N.R. (1989). The role of ion-pairs in α-helix stability – 2 new designed helical peptides. *J. Am. Chem. Soc.* **111**, 2733-2734.
33. Scholtz, J.M., Qian, H., Robbins, V.H. & Baldwin, R.L. (1993). The energetics of ion-pair and hydrogen-bonding interactions in a helical peptide. *Biochemistry* **32**, 9668-9676.
34. Yorgey, P.S. (1993). The structure and biosynthesis of microcin B17, a novel DNA gyrase inhibitor. Ph.D. Thesis, Harvard University, Cambridge.
35. Jung, G. (1991). Lantibiotics – ribosomally synthesized biologically active polypeptides containing sulfide bridges and α,β-didehydro-amino acids. *Angew. Chem. Int. Ed. Engl.* **30**, 1051-1192.
36. Vizán, J.L., Hernández-Chico, C., del Castillo, I. & Moreno, F. (1991). The peptide antibiotic microcin B17 induces double-stranded cleavage of DNA mediated by *E. coli* DNA gyrase. *EMBO J.* **10**, 467-476.
37. Cheng, J.-W., Chen, C., Huang, T.-H., Chou, S.-H. & Chen, S.-H. (1995). Conformation of the propeptide domain of factor IX. *Biochim. Biophys. Acta* **1245**, 227-331.
38. van den Hooven, H.W., Rollema, H.S., Siezen, R.J., Hilbers, C.W. & Kuipers, O.P. (1997). Structural features of the final intermediate in the biosynthesis of the lantibiotic nisin. Influence of the leader peptide. *Biochemistry* **36**, 14137-14145.
39. Sanford, D.G., Kanagy, C., Sudmeier, J.L., Furie, B.C., Furie, B. & Bachovchin, W.W. (1991). Structure of the propeptide of prothrombin containing the γ-carboxylation recognition site determined by two-dimensional NMR spectroscopy. *Biochemistry* **30**, 9835-9841.
40. Sönnichsen, F.D., Van Eyk, J.E., Hodges, R.S. & Sykes, B.D. (1992). Effect of trifluoroethanol on protein secondary structure: an NMR and CD study using a synthetic actin peptide. *Biochemistry* **31**, 8790-8798.
41. Najbar, L.V., Craik, D.J., Wade, J.D., Salvatore, D. & McLeish, M.J. (1997). Conformational analysis of LYS(11-36), a peptide derived from the β-Sheet region of T4 lysozyme, in TFE and SDS. *Biochemistry* **36**, 11525-11533.
42. Breil, B.T., Ludden, P.W. & Triplett, E.W. (1993). DNA sequence and mutational analysis of genes involved in the production and resistance of the antibiotic peptide trifolitoxin. *J. Bacteriol.* **175**, 3693-3702.
43. Lethbridge, B.J. (1989). The structure of trifolitoxin. Ph.D. Thesis, University of Adelaide, Adelaide.
44. Dunne, S.J., Cornell, R.B., Johnson, J.E., Glover, N.R. & Tracey, A.S. (1996). Structure of the membrane binding domain of CTP: phosphocholine cytidyltransferase. *Biochemistry* **35**, 11975-11984.

45. Blumenthal, D.K., *et al.*, & Krebs, E.G. (1985). Identification of the calmodulin-binding domain of skeletal-muscle myosin light chain kinase. *Proc. Natl Acad. Sci. USA* **82**, 3187-3191.
46. Takio, K., Blumenthal, D.K., Walsh, K.A., Titani, K. & Krebs, E.G. (1986). Amino-acid sequence of rabbit-muscle myosin light chain kinase. *Biochemistry* **25**, 8049-8057.
47. McCafferty, D.G., Lessard, I.A.D. & Walsh, C.T. (1997). Mutational analysis of potential zinc-binding residues in the active site of the enterococcal D-Ala-D-Ala dipeptidase VanX. *Biochemistry* **36**, 10498-10505.
48. Fields, G.B. & Noble, R.L. (1990). Solid phase peptide synthesis utilizing 9-fluorenylmethoxycarbonyl amino acids. *Int. J. Pep. Protein Res.* **35**, 161-214.
49. Cavanagh, J., Fairbrother, W.J., Palmer III, A.G. & Skelton, N.J. (1996). *Protein NMR Spectroscopy*, Academic Press, San Diego.
50. Ludvigsen, S. & Poulsen, F.M. (1992). Positive theta-angles in proteins by nuclear magnetic resonance spectroscopy. *J. Biomol. NMR* **2**, 227-233.
51. Freedman, S.J., Sanford, D.G., Bachovchin, W.W., Furie, B.C., Baleja, J.D. & Furie, B. (1996). Structure and function of the epidermal growth factor domain of P-selectin. *Biochemistry* **35**, 13733-13744.
52. Freedman, S.J., Furie, B.C., Furie, C. & Baleja, J.D. (1995). Structure of the calcium ion-bound γ-carboxyglutamic acid-rich domain of factor IX. *Biochemistry* **34**, 12126-12137.
53. Sambrook, J., Fritsch, E.F. & Maniatis, T. (1989). *Molecular Cloning: A Laboratory Manual*, (2nd edn), Cold Spring Harbor Laboratory, Cold Spring Harbor, NY.
54. Deng, W.P. & Nickoloff, J.A. (1992). Site-directed mutagenesis of virtually any plasmid by eliminating a unique site. *Anal. Biochem.* **200**, 81-88.